Structural and magnetic properties in Mn-doped ZnO films prepared by pulsed-laser deposition

Qiang Li [a], Yuyin Wang [b], Jiandang Liu [a], Wei Kong [a], Bangjiao Ye [a,*]

[a] State Key Laboratory of Particle Detection and Electronics, University of Science and Technology of China, No. 96, Jinzhai Road Hefei 230026, People's Republic of China
[b] National Synchrotron Radiation Laboratory, University of Science and Technology of China, Hefei 230029, People's Republic of China

ARTICLE INFO

ABSTRACT

We investigated the structural and magnetic properties of $Zn_{0.95}Mn_{0.05}O$ films prepared on sapphire substrates by pulsed-laser deposition. Only low temperature ferromagnetism (Curie temperature lower than 50 K) was observed in Mn-doped samples, while pure ZnO film shows a typical paramagnetic behavior. Structural analyses indicate that the substitutional Mn^{2+} ions play a significant role for the low temperature ferromagnetism. Lattice defects such as V_O and V_{Zn} were not proven to be effective factors for the origin of ferromagnetism in the films. The low temperature ferromagnetism might be interpreted as p–d hybridization from indirect coupling of Mn ions (Mn–O–Mn).

© 2013 Elsevier B.V. All rights reserved.

1. Introduction

ZnO-based dilute magnetic semiconductors (DMSs) were extensively investigated as a promising candidate for spintronics applications due to their outstanding characteristics such as wide-band gap and large exciton binding energy [1]. Transition-metals (TM) doping proved to be an effective way to obtain ferromagnetism (FM) in ZnO systems. Especially, Co- and Mn-doped ZnO have aroused widespread interest during the past years. However, the experimental results are always contradictory and the origin of FM has far from been established clearly. For Mn-doped ZnO system, various experimental results on magnetic behavior such as room temperature FM, low temperature FM, paramagnetism and spin-glass were reported [2–5]. On the other hand, in some works the ferromagnetism was observed in $Zn_{1-x}Mn_xO$, while the origin and reproducibility of the FM are still under debate [6–8]. For example, Ramachandrana et al. observed O vacancy-mediated room temperature ferromagnetism in Mn-doped ZnO films [9]. However, calculations from Diana et al. indicate that defects such as O vacancies lead to antiferromagnetic interactions between the Mn atoms [10].

Magnetic behaviors of Mn-doped ZnO films are strongly dependent on the growth conditions. Further studies are required to understand the magnetic mechanism of this system in detail. In the present work, we fabricated the $Zn_{0.95}Mn_{0.05}O$ films under low and high oxygen pressure on sapphire substrates by pulsed-laser deposition, and then annealed the films under nitrogen atmosphere at 700 °C. The correlation between structural features and magnetic properties was characterized clearly.

2. Experiments

Pure and Mn-doped ZnO films were deposited on Al_2O_3 (0 0 0 1) single crystals by pulsed laser deposition technique. $Zn_{0.95}Mn_{0.05}O$ target was prepared by solid state reaction method from ZnO and MnO_2 powders. Mixed powders were ground in agate mortar for 6 h, and then sintered at 500 °C for 16 h. Target sintered under 500 °C was proved to be suitable for growing ferromagnetic Mn-doped ZnO films [11]. Deposition process was using pulsed KrF excimer laser ($\lambda = 248$ nm) with a repetition rate of 5 Hz and energy of 200 mJ/pulse. During the process the substrate temperature was keep at 550 °C. Oxygen partial pressure for Mn-doped ZnO films was 2×10^{-4} Pa and 10 Pa, respectively. The undoped ZnO film was prepared under oxygen pressure of 2×10^{-4} Pa. The time of deposition was 20 min and the thickness of films was 260 nm estimated by stylus profilometer. Magnetic properties of the films were measured using vibrating sample magnetometer (VSM). The X-ray diffraction (XRD) and X-ray photoelectron spectroscopy (XPS) were used to investigate crystal structures and chemical valence states, respectively. Defect characterization was performed by Positron annihilation spectroscopy and Raman spectroscopy.

* Corresponding author. Tel.: +86 0551 63607404.
E-mail address: bjye@ustc.edu.cn (B. Ye).
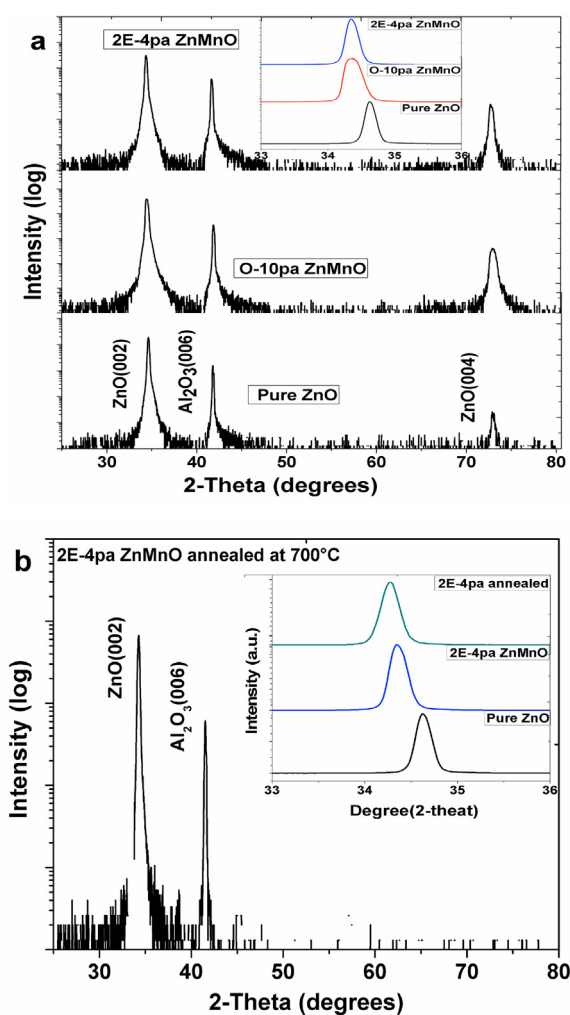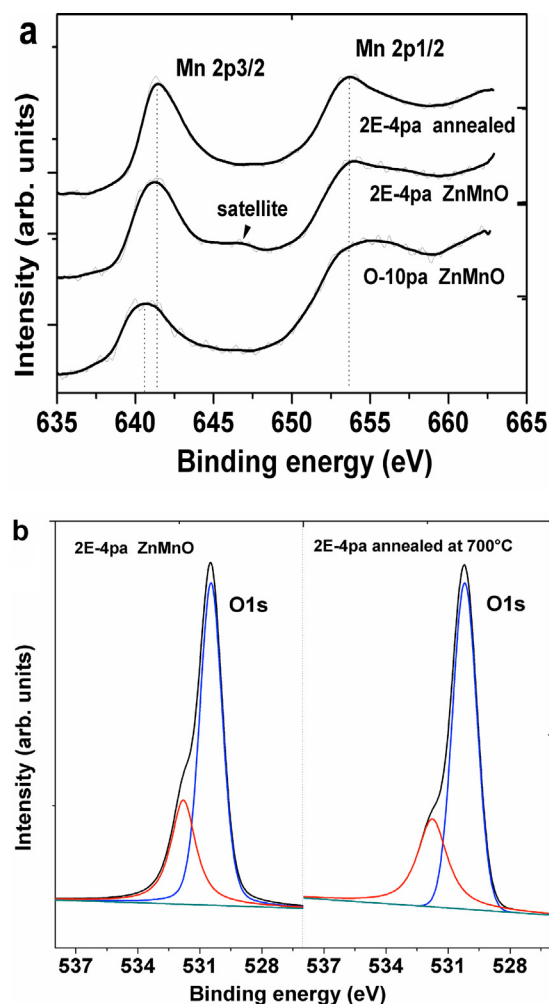
Fig. 1. The XRD patterns of (a) pure and Mn-doped ZnO films, (b) 2×10^{-4} Pa prepared $Zn_{0.95}Mn_{0.05}O$ film annealed at 700 °C. The insets in (a) and (b) are enlarged region of ZnO (0 0 2) peak of those films.

Fig. 2. XPS spectra of (a) Mn 2p for Mn-doped ZnO films, (b) O 1s for as-prepared and annealed 2×10^{-4} Pa $Zn_{0.95}Mn_{0.05}O$ film.

3. Results and discussion

Fig. 1(a) displays the XRD patterns of the grown films. In addition to substrate diffraction, only (0 0 2) and (0 0 4) peak of wurtzite hexagonal ZnO was detected. No evidence of Mn-related second phases was observed within the detection limit of XRD, indicating a general solution of Mn ions into ZnO lattices. Diffraction peak of ZnO (0 0 2) was found to shift slightly to lower angles after Mn-doped (inset in Fig 1(a)). It is generally considered that the radius of Mn ions (83 pm) is larger than that of Zn ions (74 pm), thus substitution of Mn ions at Zn site can increase the lattice constant on c-axis [12]. For the $Zn_{0.95}Mn_{0.05}O$ film prepared under 2×10^{-4} Pa, no separation of Mn-cluster phases was detected after annealing at 700 °C, as shown in Fig. 1(b). It is possibly interpreted as the solubility limit of Mn ions in ZnO lattices is much larger than 5 at% [13]. Inset in Fig. 1(b) display a further left shift of (0 0 2) peak after annealing, indicating an improved occupancy of Mn ions into ZnO lattices.

XPS measurements were employed to further characterize the chemical bonding states of Mn in films, as shown in Fig. 2(a). The binding energy of Mn 2p1/2 peaks are located at about 653.6 eV overlap with an auger peak of Zn (656.7 eV). The Mn 2p3/2 peaks are located at 640.3 eV, 640.8 eV and 640.9 eV for $Zn_{0.95}Mn_{0.05}O$ films prepared under 10 Pa, 2×10^{-4} Pa, as well as the annealed 2×10^{-4} Pa film at 700 °C, respectively. It indicates that the doped

Mn ions in the films are dominantly in divalent states [14]. No binding energy peaks of metallic Mn (637.7 eV) and Mn^{4+} ions (642.6 eV) were detected within the limitation of XPS. Besides of the slight shift of the 2p3/2 peak, the peak linewidth also show slightly narrower for 2×10^{-4} Pa prepared film, and a further decrease of linewidth was found after annealing at 700 °C. It is considered that the chemical states surrounding Mn^{2+} ions are more inclined to Mn–O bonding for this film, or the dopant-induced lattice defects were adjusted after annealing and more Mn^{2+} ions into stable substitutional combination. This is consistent with the results of XRD. Fig. 2(b) displays the asymmetric O1s peaks of as-grown and annealing $Zn_{0.95}Mn_{0.05}O$ film prepared under 2×10^{-4} Pa. Both the experimental peaks can be fitted by two Gaussian curves. The low binding energy peak (blue curves) located at 530 eV is attributed to lattice O^{2-} ions in wurtzite structure of ZnO, and the high binding energy peak (red curves) located at 531.8 eV is related to the oxygen deficient regions (oxygen vacancies) [15]. It can be seen that after annealing the high binding energy peak shows decrease both in the intensity and relative area. This result indicates that annealing at high temperature improved the lattice quality and resulted in the decrease of oxygen vacancy concentration, which consistent with the previous reports [16].

Fig. 3 display the room temperature Raman spectra range from $200 \, cm^{-1}$ to $900 \, cm^{-1}$. A volume of 514.5 nm line from an Ar^+ ion laser was used for excitation. In addition to the substrate phonon modes of $420 \, cm^{-1}$ and $752 \, cm^{-1}$, the expected ZnO modes locate

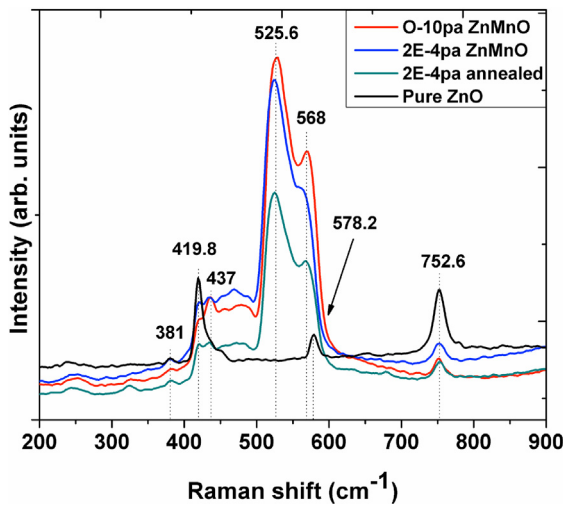Fig. 3. Room-temperature Raman spectra of pure ZnO film and $Zn_{0.95}Mn_{0.05}O$ films.

Fig. 4. The S-parameter as a function of positron implantation energy for pure and Mn-doped ZnO films.

at 381 cm^{-1} [A_1 transverse optical mode (A_1^{TO})], 437 cm^{-1} [high frequency branch of E_2 (E_2^{high})], 568 cm^{-1} [A_1 longitudinal optical mode (A_1^{LO})] and 578.2 cm^{-1} [E_1 longitudinal optical mode (E_1^{LO})] were also detected. Compared with the pure ZnO, no peak located at 578.2 cm^{-1} was evidently observed in Mn-doped films. It is considered that the 578.2 cm^{-1} peak was overwhelmed by the strong additional peak located at 568 cm^{-1}, which may be induced by oxygen-related vacancies [17]. Besides the intrinsic peaks of ZnO, an additional strongest mode located at 525.6 cm^{-1} was also observed in Mn-doped films. Although this mode was considered as a local vibration of Mn in ZnO, the vicinal line was also observed in Sb- and Ce-doped ZnO samples [18,19]. Therefore, this vibration mode is more likely related to the Mn-doping induced lattice defects of ZnO, as the previous reports suggested [20]. The relative intensity of 525.6 cm^{-1} peak in the Mn-doped films is consistent with that of 568 cm^{-1} mode. It is indicates that the O-related vacancies or defects in the 2×10^{-4} Pa prepared film obviously decreased after annealed at 700 °C.

The V_{Zn}-related defects in our films were characterized by slow positron annihilation spectroscopy, which was proved to be a sensitive tool for detecting the cationic defects in materials [21]. Positrons are easily trapped by vacancy defects, result in a narrowing of 511 keV annihilation peak compared to bulk annihilation. S parameter was defined as a fraction of counts in the central region of this 511 keV peak [22]. Therefore, positrons annihilated in vacancies will result in an increase in S-parameters. In our experiments, the depth profile of V_{Zn}-related defects was measured by mono-energetic positron beam with energies varying from 0.5 keV to 20 keV. The S-parameter as a function of incident positron energy for pure and Mn-doped ZnO films was shown in Fig. 4. Based on VEPFIT fitting, the curves for all the films can be divided into three layers. The surface layer with positron energy range of 0–1.5 keV usually exhibit high S-parameters due to the formation of positronium atoms at material surface [23]. The energy range of 1.5–9 keV corresponds to the sample layer of ZnO films. A tempered slope change was observed at 9 keV, indicating the interface of film and substrate. Positrons annihilate mainly in the sapphire substrate after the incident energy above 9 keV. Compared with the sample layer of pure ZnO, significant increase of S-parameters was observed in Mn-doped ZnO films. It is worth noting that this increase of S-parameters was not observed in Co-doped ZnO films, despite the identical preparation conditions and doping concentration. Considering that the radius of Co ions (74.5 pm) is much close to the Zn ions (74 pm), it is reasonable to attribute the increase of S-parameters to Mn-doping induced lattice defects in ZnO films,

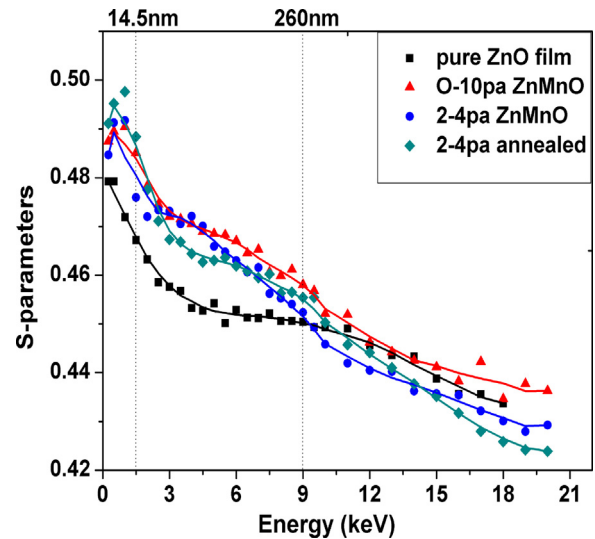since the radius of Mn^{2+} ions are much larger than Zn^{2+} ions. After annealing, the S-parameters of 2×10^{-4} Pa prepared $Zn_{0.95}Mn_{0.05}O$ film slightly decrease. It indicates that V_{Zn}-related defects were reduced after this sample was annealed at 700 °C. While the substitutional Mn^{2+} ions induced lattice expansion cannot be eliminated by annealing.

Field-dependent magnetization (M–H) curves for the Mn-doped films clearly show paramagnetic behavior at room temperature and 50 K, as shown in Fig. 5(a) and (b). Note that the diamagnetic backgrounds have not been subtracted from those curves. For the $Zn_{0.95}Mn_{0.05}O$ film prepared under 10 Pa, a clear hysteresis loop superimposed on the background was detected at 10 K (Fig. 5(c)). The temperature dependent magnetization (M–T) curves in Fig. 5(d) display a rapid decrease with the increase of temperature from 5 K to 35 K, and then almost flat with temperature above 50 K. The field-cooling and zero field-cooling curves overlap with each other at low temperature, indicating an absence of spin glass or superparamagnetic states in the film [24]. M–H and M–T results reveal that only low temperature ferromagnetism (LTFM) exist in our films with the Curie temperature no more than 50 K. The 2×10^{-4} Pa prepared $Zn_{0.95}Mn_{0.05}O$ film show clear ferromagnetic curve at 10 K. After annealing, this ferromagnetic curve shows an obvious increase both in saturation magnetization (M_S) and coercive field (H_C).

Although V_{Zn}-induced room temperature FM in ZnO was reported [6], the zinc vacancies cannot as the origin of the low temperature FM in our films, since the V_{Zn}-related defects in 2×10^{-4} Pa prepared $Zn_{0.95}Mn_{0.05}O$ film were reduced after annealing at 700 °C while the FM show a further increase in M_S and H_C. It is may considered that the content of V_{Zn} in the films is relatively low, thus no long-range magnetic orders were formed among those zinc vacancies. Likewise, annealing induced decrease of oxygen vacancies in the films. V_O mediated room temperature FM in Mn-doped ZnO samples was characterized in previous reports, which is depicted by a bound magnetic polaron (BMP) mechanism [9,17]. While this mechanism is not confirmed in our experiments, since the oxygen vacancies and low temperature FM show inconsistent changes in annealing behavior. Calculations from Diana et al. suggested that the oxygen vacancies may lead to antiferromagnetic interaction between Mn ions in ZnO sample, and the Curie temperature for 5% Mn-doped ZnO sample is normally lower than 50 K simulated by Monte Carlo method, which is typically consistent with our experimental results [10]. We calculated the magnetic interaction of Mn
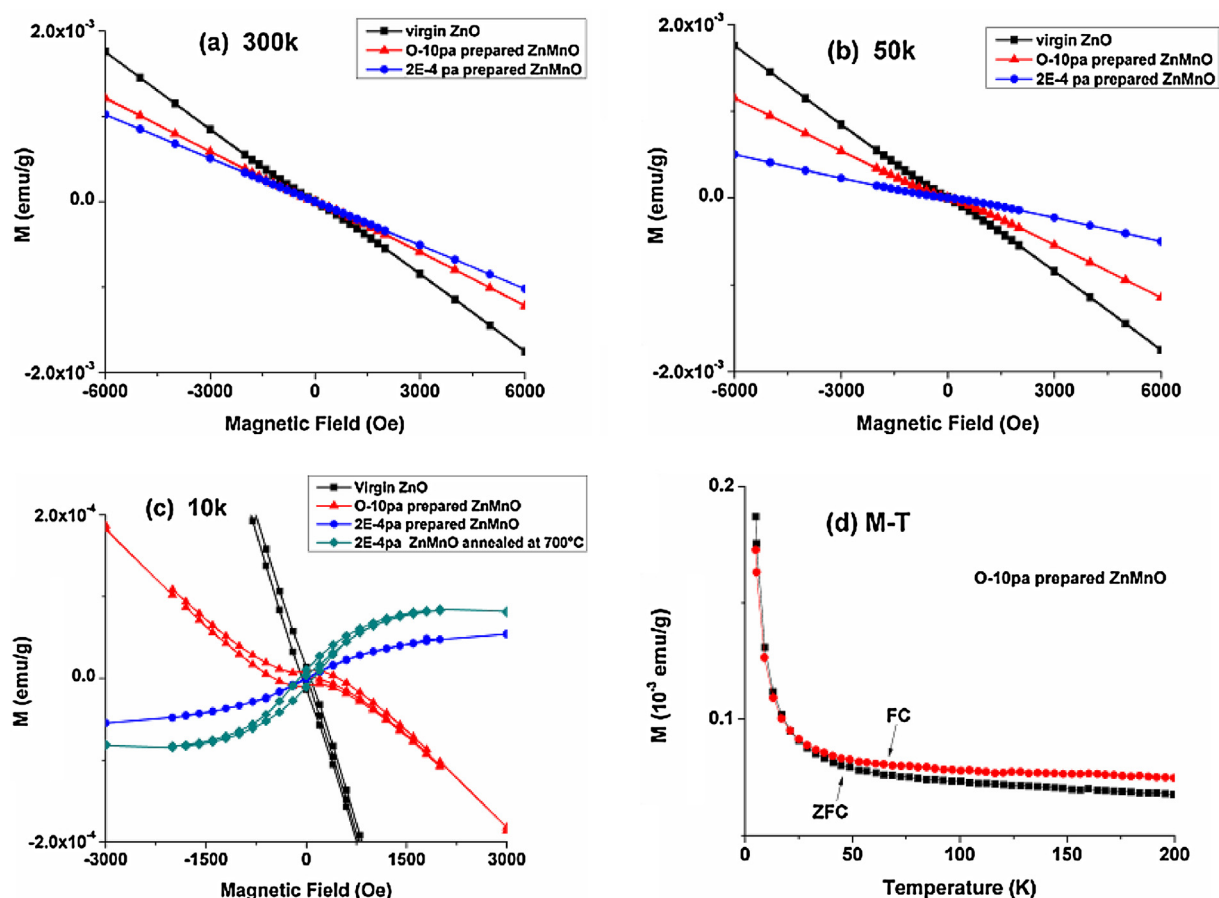
Fig. 5. The field-dependent magnetization (*M*–*H*) curves measured at (a) room temperature, (b) 50 K and (c) 10 K for pure and Mn-doped ZnO films. (d) Temperature dependent magnetization measured in field-cooling and zero field-cooling (FC/ZFC) under 500 Oe for 10 Pa prepared $Zn_{0.95}Mn_{0.05}O$ film.

ions in the ZnO using generalized gradient approximation (GGA) and GGA + U (Coulomb interaction) method of density functional theory. The results indicate that introducing of V_O in Mn–Mn cannot reverse the ground energy from anti-FM to FM, while increase the energy gap and lead to a more stable state of antiferromagnetism. Given the results of XRD measurement, Mn^{2+} ions substituted at Zn site may play an important role in the origin of this low temperature FM. Different from the direct interaction of Mn–Mn, the indirect coupling between Mn ions (Mn–O–Mn) may result in ferromagnetic order [12]. The p–d hybridization from indirect coupling of Mn ions (Mn–O–Mn) was reinforced after annealing due to the decrease of V_O content [12], which is considered as the reason of LTFM increase in our films. It seems that the LTFM mechanism is far from the defect such as V_{Zn} or V_O induced (or mediated) room temperature FM in Mn-doped ZnO. Different mechanisms existed in Mn-doped ZnO samples may lead to a variety of magnetic behavior in previous experimental results.

4. Summary

In summary, pure ZnO and $Zn_{0.95}Mn_{0.05}O$ films were prepared by pulsed-laser deposition technique. Magnetic measurements indicate that the Mn-doped ZnO films only show low temperature hysteresis loop at 10 K. After annealing, the doping induced defects (such as V_{Zn} and V_O) clearly decrease while the FM shows increase both in M_S and H_C. It indicates that the LTFM observed in the films not origin from zinc vacancies or mediated by oxygen vacancies. XRD results show an improved occupancy of Mn^{2+} ions at Zn^{2+} site after annealing. The substitutional Mn^{2+} ions may play an important role in the origin of the LTFM in the films, which

is possibly attributed to the indirect interaction coupling of those substitutional Mn^{2+} ions.

References

[1] R. Kumar, F. Singh, B. Angadi, J.W. Choi, W.K. Choi, K. Jeong, J.H. Song, M.W. Khan, J.P. Srivastava, A. Kumar, R.P. Tandon, J. Appl. Phys. 100 (2006) 113708.
[2] D. Mukherjee, P. Mukherjee, H. Srikanth, S. Witanachchi, J. Appl. Phys. 111 (2012) 07C318.
[3] J. Jin, X.Y. Zhang, X.Y. Zhou, G.S. Chang, Semicond. Sci. Technol. 27 (2012) 035012.
[4] J. Alaria, P. Turek, M. Bernard, M. Bouloudenine, A. Berbadj, N. Brihi, G. Schmerber, S. Colis, A. Dinia, Chem. Phys. Lett. 415 (2005) 337–341.
[5] T. Fukumura, Z. Jin, M. Kawasaki, T. Shono, T. Hasegawa, S. Koshihara, Appl. Phys. Lett. 78 (2001) 958.
[6] Wensheng Yan, Zhihu Sun, Qinghua Liu, Zhongrui Li, Zhiyun Pan, Jie Wang, Shiqiang Wei, Dan Wang, Yingxue Zhou, Xinyi Zhang, Appl. Phys. Lett. 91 (2007) 062113.
[7] V.K. Sharma, G.D. Varma, J. Appl. Phys. 102 (2007) 056105.
[8] D. Mukherjee, T. Dhakal, H. Srikanth, P. Mukherjee, S. Witanachchi, Phys. Rev. B: Condens. Matter 81 (2010) 205202.
[9] S. Ramachandrana, J. Narayan, J.T. Prater, Appl. Phys. Lett. 88 (2006) 242503.
[10] D. Iuşan, B. Sanyal, O. Eriksson, J. Appl. Phys. 101 (2007) 09H101.
[11] P. Sharma, A. Gupta, K.V. Rao, F.J. Owens, R. Sharma, R. Ahuja, J.M. Osorio Guillen, B. Johansson, G.A. Gehring, Nat. Mater. 2 (2003) 673.
[12] U. Ilyas, R.S. Rawat, T.L. Tan, P. Lee, R. Chen, H.D. Sun, Li Fengji, Sam Zhang, J. Appl. Phys. 111 (2012) 033503.
[13] H.K. Yadav, K. Sreenivas, V. Gupta, J. Appl. Phys. 99 (2006) 083507.
[14] Z.B. Gu, C.S. Yuan, M.H. Lu, J. Wang, D. Wu, S.T. Zhang, S.N. Zhu, Y.Y. Zhu, Y.F. Chen, J. Appl. Phys. 98 (2005) 053908.

[15] M. Naeem, S.K. Hasanain, M. Kobayashi, Y. Ishida, A. Fujimori, Scott Buzby, S. Ismat Shah, Nanotechnology 17 (2006) 2675–2680.
[16] W. Yan, Q. Jiang, Z. Sun, T. Yao, F. Hu, S. Wei, J. Appl. Phys. 108 (2010) 013901.
[17] Q.Q. Gao, Q.X. Yu, K. Yuan, X.N. Fu, B. Chen, C.X. Zhu, H. Zhu, Appl. Surf. Sci. 264 (2013) 7–10.
[18] C. Bundesmann, N. Ashkenov, M. Schubert, D. Spemann, T. Butz, E.M. Kaidashev, M. Lorenz, M. Grundmann, Appl. Phys. Lett. 83 (2003) 1974.
[19] B.C. Cheng, Y.H. Xiao, G.S. Wu, L.D. Zhang, Appl. Phys. Lett. 84 (2004) 416.
[20] J.B. Wang, G.J. Huang, X.L. Zhong, L.Z. Sun, Y.C. Zhou, E.H. Liu, Appl. Phys. Lett. 88 (2006) 252502.
[21] R. Krause-Rehberg, H.S. Leipner, Positron Annihilation in Semiconductors, Defect Studies (Springer Series in Solid-State Sciences, 127, Springer, Berlin, 1999.
[22] J. Toivonen, T. Hakkarainen, M. Sopanen, H. Lipsanen, J. Oila, K. Saarinen, Appl. Phys. Lett. 82 (2003) 1.
[23] B.Y. Zhang, et al., Appl. Phys. Lett. 99 (2011) 182503.
[24] T. Fukumura, Z. Jin, M. Kawasaki, T. Shono, T. Hasegawa, S. Koshihara, H. Koinuma, Appl. Phys. Lett. 78 (2001) 958.